Combination of CP/MAS NMR Spectroscopy and X-ray Crystallography: Structure and Dynamics in Molecular Crystals of Hydrogen, Lithium, Sodium, Rubidium, and Cesium Penicillin V

Michaela Wendeler,[†] Jamila Fattah,[†] J. Mark Twyman,[†] Alison J. Edwards,[‡,§,#] Christopher M. Dobson,*[,†,§] Stephen J. Heyes,*[,†] and Keith Prout*[,‡,§]

Contribution from the Inorganic Chemistry Laboratory, South Parks Road, Oxford OX1 3QR, U.K., the Chemical Crystallography Laboratory, 9 Parks Road, Oxford OX1 3PD, U.K., and the Oxford Centre for Molecular Sciences, South Parks Road, Oxford, OX1 3QT U.K.

Received November 25, 1996. Revised Manuscript Received June 4, 1997[⊗]

Abstract: ^{13}C CP/MAS NMR spectra of the free acid of phenoxymethyl penicillin (penicillin V) and of its lithium, sodium, rubidium, and cesium salts ($C_{16}H_{17}N_2O_5SM$, M = H, Li·H_2O, Na, Rb, and Cs) have been studied at a range of temperatures between 180 and 400 K. The ^{13}C CP/MAS NMR spectra at ambient temperature indicate that the structures have one, two, one, four, and one molecule(s), respectively, in the crystallographic asymmetric unit. This is confirmed by the known crystal structure of the free acid and the single-crystal X-ray diffraction studies reported here of the various salts. The variable-temperature ^{13}C CP/MAS NMR spectra indicate that the phenyl rings of all the molecules perform 180° flips about their local C_2 axes, with measured or extrapolated rate constants in the range 5×10^{-12} to 8×10^{9} s^{-1} in the temperature regime 200−380 K, and spanning 11 orders of magnitude at ambient temperature. The atomic displacement parameters of the X-ray structural model suggest that these rings also undergo significant in-plane librations. The Arrhenius activation parameters for the ring flip motions have been determined, by analysis of exchange and dipolar broadened NMR line shapes and with 1-D (and 2-D) magnetization transfer experiments, for the free acid and all four salts. The activation barriers have been interpreted in terms of the degree of entrapment of the phenyl groups and the nature of the packing interactions in the different crystal structures.

Introduction

A particularly powerful approach to the detailed characterization of local and extended structure and molecular motion in the solid state has proved to be a combination of solid-state NMR and diffraction methods. The combined use of the two techniques in the characterization of several molecular systems has, for example, facilitated a full analysis of structure and dynamics in situations where either technique in isolation would have failed to yield even a small fraction of the information provided by the combination of the two techniques(See ref 1 and references therein).

The information provided by X-ray diffraction and by NMR techniques is fundamentally different and highly complementary. Structure solution from single-crystal X-ray diffraction data[2] yields information on intramolecular structure including bond distances and conformational angles, and on intermolecular contacts and packing relationships. Similar information is encapsulated in NMR shielding parameters,[3] but the detailed information in the form typically obtained from structure solution of single-crystal X-ray diffraction data cannot be determined directly, even for small, highly crystalline molecular systems, from typical ^{13}C CP/MAS NMR spectra of microcrystalline samples. Instead, ^{13}C CP/MAS NMR is well suited to providing qualitative and semiquantitative information about local structure and only by inference from the local structural details can the nature of the extended structure be proposed.[4]

The adps from X-ray diffraction[5] contain information about translational, vibrational, and rotational (librational) oscillations of the molecule or groups within the molecule, and also on the nature of any positional disorder of atoms away from their mean positions (which may be static or dynamic in nature) and, on occasion, on the goodness of fit of the model to the diffraction data. The time scale of the diffraction technique ($\sim 10^{-18}$ s) is too short for direct detection of atomic motions that are slow on the time scale of bond vibrations. These slow dynamic processes will only be detected if they result in new atomic positions and therefore cannot be distinguished from "static" molecular disorder. When such disorder is detected the X-ray structure solution contains no direct information about the relative rates of any dynamic processes. In contrast to diffraction techniques, the utility of NMR in the elucidation of molecular dynamics arises because various NMR spectroscopic interactions are directly sensitive to motions over a wide range of time scales ($\sim 10^{2}-10^{-10}$ s) that are slow compared with that of bond vibrations; no other technique possesses such a wide range of rates over which motion may be examined explicitly.[6] Motions with time scales in the range $10^{1}-10^{-7}$ s have been

* To whom correspondence should be addressed.
† Inorganic Chemistry Laboratory.
‡ Chemical Crystallography Laboratory.
§ Oxford Centre for Molecular Sciences.
# School of Chemistry, University of Melbourne, Parkville, Vic. 3052, Australia.

⊗ Abstract published in *Advance ACS Abstracts,* September 15, 1997.

(1) (a)Fattah, J.; Twyman, J. M.; Heyes, S. J.; Watkin, D. J.; Edwards, A. J.; Prout, K.; Dobson, C. M. *J. Am. Chem. Soc.* **1993**, *115*, 5636−5650 and references therein. (b) Brouwer, E. B.; Enright, G. D.; Ripmeester, J. A. *Supramol. Chem*. **1996**, *7*, 7−9.

(2) Glusker, J. P.; Lewis, M.; Rossi, M. *Crystal Structure Analysis for Chemists and Biologists*, VCH: Weinheim, 1994.

(3) Harris, R. K. *Nuclear Magnetic Resonance Spectroscopy*, rev. ed.; Longman: London, 1986.

(4) Clayden, N. J.; Dobson, C. M.; Lian, L.-Y.; Twyman, J. M. *J. Chem. Soc., Perkin Trans. II* **1986**, 1933−1940.

(5) Dunitz, J. D.; Maverick, E. F.; Trueblood, K. N. *Angew. Chem., Int. Ed. Engl.* **1988**, *27*, 880−895.

(6) Muetterties, E. L. *Inorg. Chem.* **1965**, *4*, 769−771.

S0002-7863(96)04065-6 CCC: $14.00

studied in the present case through the direct sensitivity of ^{13}C CP/MAS NMR experiments to magnetization transfer, exchange-broadening, and dipolar broadening time scales. NMR is particularly useful in its sensitivity to these relatively slow dynamic processes. We applied this approach to a study of the potassium penicillin V (KpenV) system. The combination of ^{13}C CP/MAS NMR with X-ray crystallography was fundamental to the elucidation of the complexities of the low-symmetry structure and its dynamically induced phase transition.[1a] In this work we extend the study of the penV system to the crystalline Li-, Na-, Rb-, and CspenV and the free acid (HpenV). The penV series was chosen for study because particular questions are raised from examination of the information already available. The structure of KpenV is unusual with four molecules in the asymmetric unit and, although related to the previously known HpenV structure,[7] the differences appear to be due to the different coordination demands of the cation; the present study considers systematically the effect that the size of the cation has on the crystal structure. A feature of previous ^{13}C CP/MAS NMR studies of a variety of penicillins is the detection of dynamic averaging effects, notably those associated with 180° flips of the phenyl rings in side chains about their C_2 axes. The present study enables the frequency of these ring flips to be characterized in a closely related set of packing environments. The methodical comparison offers an opportunity to examine the balance of effects on the rate of phenyl ring flips, not just the influence of direct interactions with local environment but also of the flexibility in that local environment conferred by features of the long-range ordering motif. From this study insight will be gained into the general aspects of spatially demanding, slow motions in molecular solids.

Experimental Section

i. Preparation and Characterization of H^+, Li^+, Na^+, Rb^+, and Cs^+ Salts of 6-(Phenoxyacetamido)penicillanic Acid (PenV). The lithium (LipenV), sodium (NapenV), rubidium (RbpenV), and cesium (CspenV) salts of 6-(phenoxyacetamido)penicillanic acid (HpenV) were prepared by ion exchange from the free acid and recrystallized by vapor diffusion.

HpenV. HpenV (Sigma Chemical Co.) was recrystallized by the vapor diffusion of acetone into an aqueous alcohol solution. Crystal formation was observed after 5 h, and the crystals were collected by filtration after 2 days and dried in air.

Li-, Rb-, and CspenV. Solutions of HpenV (3.50 g, 10 mmol) in THF (12 mL) and distilled H_2O (1 mL) were adjusted to pH ~5 with the dropwise addition of 4% LiOH/5% RbOH/3% CsOH. The samples were lyophilized to give LipenV, 2.93 g, 78.3%/RbpenV 3.34 g, 76.8%/CspenV, 4.259 g, 88.3%. For recrystallization, MpenV (300 mg) was dissolved in distilled water (Li, 0.6 mL; Rb, 0.3 mL; Cs 0.25 mL). Ethanol (Li, 0.6 mL; Rb, 0.3 mL; Cs, 4 mL) and 2-propanol (Li, 2 mL; Rb, 0.2 mL; Cs, 0.8 mL) were added dropwise. Flasks were left to stand in ethanol (Li and Cs) or acetone (Rb) baths, and crystal growth in the form of fine needles was observed after ~2 d. The material was then subjected to *two* further similar recrystallizations, and the final crystals were collected by filtration and air-dried. In contrast with other penV salts the samples of LipenV contain water of crystallization; all procedures used to prepare and recrystallize LipenV resulted in one crystalline form, the monohydrate. The water is lost progressively on heating above 340 K, but the crystals rehydrate on standing in the atmosphere, (Figure S1). (Figures S1−S11 are in the Supporting Information). Elemental analyses: (LipenV) Found C 51.54, H 5.44, N 7.49, S 8.48, Li 1.90 $C_{16}H_{17}LiN_2O_5S{\cdot}H_2O$; requires C 51.34, H 5.12, N 7.48, S 8.57, Li 1.85. (RbpenV) Found C 44.8, H 3.95, N 6.53, Rb 17.82 $C_{16}H_{17}N_2O_5RbS$; requires C 44.19, H 3.94, N 6.44, Rb 19.65. (CspenV) Found C 39.82, H 3.48, N 5.79, Cs 25.17 $C_{16}H_{17}CsN_2O_5S$; requires C 39.84, H 3.55, N 5.81, Cs 27.56.

NapenV. A solution of HpenV (2.00g, 5.71 mmol) in THF (8 mL) and distilled H_2O (3 mL) was adjusted to pH ~5 with 2.5% NaOH, and the excess THF was removed under reduced pressure. The sample was lyophilized to give NapenV, 1.83 g, 86%. NapenV (500 mg) was dissolved in distilled water (0.8 mL), and 2-propanol (0.15 mL) added dropwise. The flask was left to stand in an acetone bath, and crystal growth in the form of fine needles was observed after 1 h. The crystals (440 mg) were collected by filtration after three days and dried in air. Elemental analysis: Found: C 51.50, H 4.64, N 7.46, S 8.52, Na 5.91 $C_{16}H_{17}N_2NaO_5S$, requires C 51.61, H 4.60, N 7.52, S 8.61, Na 6.17.

Microanalyses were performed by the analytical service of the Inorganic Chemistry Laboratory. C, H, and N contents were determined by combustion analysis and metal analyses by atomic absorption spectroscopy.

For each compound selected crystals were used for the single-crystal X-ray diffraction analysis. The same batch of the compound, ground into a finely divided powder, was used for the CP/MAS NMR experiments. The X-ray powder diffractograms obtained from the samples used for the CP/MAS NMR experiments were compared with those computed (LAZY PULVERIX[8]) from the cell dimensions and atomic parameters observed by single-crystal diffraction work and confirmed that the X-ray diffraction and NMR experiments were carried out on the same polymorphic form.

ii. Single-Crystal X-ray Diffraction. Relevant details of the crystallography for LipenV, NapenV, and CspenV are given in Table 1 and more extensively in the Supporting Information Table S1. Data reduction included Lorentz and polarization corrections. All three structures were solved by direct methods[9] which yielded all non-hydrogen atom positions for each of the three salts. Positional and first isotropic then atomic displacement parameters for the non-hydrogen atoms were refined to convergence by the least-squares method, minimizing $\sum w(F_{obs} - F_{calc})^2$ for all observed reflections. The full normal matrix was used together with a Chebyshev polynomial weighting scheme,[10] the parameters for which are given in Table S1. For all three structures an empirical absorption correction (DIFABS[11]) was applied prior to the final refinement cycles. Hydrogen atoms were included in the models at geometrically idealized positions. Final residuals are given in Table 1. For the lithium salt, which is a hydrate, the lithium ion and the water molecule could not be distinguished in the interpretation of the electron density maps until after the beginning of the anisotropic refinement.

Except where indicated to the contrary, the Oxford CRYSTALS[12] system was used for all crystallographic calculations and CAMERON[13] for crystallographic drawings. Scattering factors were taken from Cromer and Weber.[14] The atomic coordinates, atomic displacement parameters, bond distances and angles, and interionic contact and H-bond distances, Tables 2−4, are available as Supporting Information.

An X-ray structure analysis of RbpenV is in progress.[15]

iii. Solid-State NMR Spectroscopy. ^{13}C CP/MAS NMR spectra were acquired on a Bruker MSL 200 spectrometer equipped with an Oxford Instruments 4.7 T wide-bore (98 mm) superconducting solenoid

(7) Abrahamsson, S.; Hodgkin, D. C.; Maslen, E. N. *Biochem. J.* **1963**, *86*, 514−535.

(8) Yvon, K.; Jeitschko, W.; Parthe, E. LAZY PULVERIX. *J. Appl. Crystallogr.* **1977**, *10*, 73−74.

(9) Sheldrick, G. M. in *Crystallographic Computing 3*; Sheldrick, G. M., Kruger, C., Goddard, R., Eds.; Oxford University Press: Oxford, 1985; pp 175−189.

(10) Carruthers, J. R.; Watkin, D. J. *Acta Crystallogr.* **1979**, *A35*, 698−699.

(11) Walker, N.; Stuart, D. *Acta Crystallogr.* **1983**, *A39*, 158−166.

(12) Watkin, D. J.; Carruthers, J. R.; Betteridge, P. W. *CRYSTALS User Guide*, Chemical Crystallography Laboratory, Oxford. 1985.

(13) Pearce, L. J.; Prout, K.; Watkin, D. J. *CAMERON User Guide*, Chemical Crystallography Laboratory, Oxford, 1994.

(14) Cromer, D. T.; Weber, J. T. *International Tables for X-ray Crystallography*, Ibers, J. A., Hamilton, W. C., Eds.; Kynoch Press: Birmingham, 1974; Vol. 4.

(15) The diffraction patterns of crystals of RbpenV at 100 K (a = 9.460(2), b = 12.485(3), c = 15.105(3) Å, α = 92.88(2), β = 99.16(2), γ = 90.40(2)°, V = 1758.8 Å^3), 293.4 K (a = 9.505(2), b = 12.622(3), c = 15.363(3) Å, α = 93.81(2), β = 98.85(3), γ = 90.19(2)°, V = 1817.0 Å^3), and 370 K (a = 9.530(4), b = 6.335(1), c = 15.488(3) Å, α = 94.18(2), β = 98.86(2), γ = 90.16(2)°, V = 921.3 Å^3) have been recorded. A detailed examination of these diffraction patterns shows that RbpenV is essentially isomorphous and isostructural with KpenV both above and below the phase change at ~365 K.

Table 1. Crystal Data and Refinement Parameters

crystal and experimental data	LipenV	NapenV	CspenV
formula	$C_{16}H_{17}LiN_2O_5S\cdot H_2O$	$C_{16}H_{17}N_2NaO_5S$	$C_{16}H_{17}CsN_2O_5S$
M_r	374.34	372.37	450.23
crystal system	orthorhombic	monoclinic	orthorhombic
temperature, K	295(2)	293(2)	295(2)
a, Å	7.425(1)	8.841(1)	6.5436(4)
b, Å	21.777(2)	6.129(7)	9.6181(7)
c, Å	22.677(2)	15.929(2)	30.011(2)
α, deg	90	90	90
β, deg	90	97.43	90
γ deg	90	90	90
cell vol deg Å^3	3667	856	1888.8
Z	8	2	4
D_c, g cm^{-3}	1.356	1.45	1.583
space group	$P2_12_12_1$ (no. 19)	$P2_1$ (no. 4)	$P2_12_12_1$ (no. 19)
radiation	Cu Kα	Cu Kα	Cu Kα
λ, Å	1.5418	1.5418	1.5418
no. observed ($I \geq 3\sigma I$)	2011	1746	2330
μ, cm^{-1}	18.29	21.6	158.7
final R,[a] R_w[b]	0.049, 0.055	0.038, 0.043	0.036, 0.043

[a] $R = \sum(|F_o| - |F_c|)/\sum|F_o|$. [b] $R_w = \{\sum[w(|F_o| - |F_c|)^2]/\sum[w|F_o|^2]\}^{1/2}$.

magnet operating at frequencies of 50.32 and 200.13 MHz for ^{13}C and ^{1}H, respectively. CP/MAS spectra were recorded using a double-bearing magic-angle sample spinning probe (Bruker Z32-DR-MAS-7DB), utilizing dry nitrogen for all gas requirements. Approximately 250 mg of sample was packed into 7 mm zirconia rotors with Kel-F caps for MAS at typical rates of 1−4 kHz. A single contact spin−lock cross polarization (CP) sequence[16] was used with alternate cycle spin−temperature inversion[17], with flip-back of ^{1}H magnetization[18] and with proton rf fields of ∼1.7 mT, resulting in a 90° pulse length of 3.5−4.5 μs ($\nu_{1H} \approx$ 55−75 kHz). Temperature measurement and regulation, utilizing a Bruker B-VT1000 unit equipped with a copper−constantan thermocouple and digital reference, was of the bearing gas. Temperature calibration was achieved as described previously.[1a] Spectra were generally recorded with 3−5 K temperature increments and ∼30 min was allowed for equilibration at each new temperature before commencement of spectral acquisition. Free induction decays were defined by ∼2−4 K data points over a spectral width of 20 kHz and were zero-filled to 16 K data points prior to Fourier transformation. Typically 100−1000 transients, with a CP contact time of 0.75 or 2.5 ms and a relaxation delay of 3.5−8 s, were accumulated for each spectrum. Chemical shifts are reported with respect to δ(TMS) = 0 ppm and were referenced externally to the upfield resonance of solid adamantane at 29.5 ppm.[19] Nonquaternary Supression (NQS) dipolar dephasing experiments[20] were carried out using delays of 20−200 μs.

Rotationally asynchronous, TPPI phase-sensitive CP/MAS 2D-exchange NMR experiments with mixing times in the range 2−3 s were performed as described previously.[23] 1D-magnetization-transfer measurements used the rotationally synchronized, selective experiment of Conner *et al.*[24] and were analyzed following the procedure of Jeener *et al.*[25] Exchange-broadened ^{13}C CP/MAS NMR lineshapes were simulated using the program DNMR4 (QCPE no. 466).[26] Dipolar broadening[27] was analyzed through the deconvoluted line width, $\Delta\nu_{1/2}'$, the difference between the measured and limiting line widths. A plot of $\ln(\Delta\nu_{1/2}')$ vs $(1/T)$ was fit, through a least-squares, error-weighted procedure, to the theory of Rothwell and Waugh.[27] Identification of the temperature of maximum broadening, as indicated by the best fit equation, at which the modified rate of the two-site ring flip exchange process is $4\pi\nu_{1H}$, enables the line widths to be converted to rate constants, and these constants are included in the full Arrhenius analyses. Rate data from magnetization-transfer experiments, exchange broadening simulations, and dipolar broadening analysis are all quoted in the form of modified rate constants, k ($= 2k_{AB}$ for the equipopulated two-site exchange processes studied in this work),[25] and were used to determine Arrhenius activation parameters from best fits for ln k vs $(1/T)$.

Results

a. X-ray Structure Analysis. The crystal structures of LipenV, NapenV, and CspenV have been determined in this work. Structures of KpenV at temperatures above and below the phase change occurring between 356 and 366 K have been reported by us in a previous paper.[1a] The crystal data[15] for RbpenV above and below the apparent phase change shown by NMR indicate that both forms are isomorphous with the corresponding forms of KpenV. The crystal structure of HpenV was determined by Abrahamsson *et al.*[7] The HpenV coordinates were transformed to give the correct absolute configuration. The chemical formula of penV is given in **1**; the notation, which is used in the discussion of the NMR results, is in accordance with conventions used in penicillin chemistry.

The crystal and molecular structures with atomic displacement ellipsoids are shown for CspenV, NapenV, and LipenV in Figures 1−3. Similar diagrams for KpenV are given in ref 1a. The crystal structure of HpenV is redrawn in Figure 4 from the transformed coordinates of Abrahamsson *et al.*[7] The asymmetric units of the crystal structures of HpenV, NapenV, and CspenV each contain one anion and one cation, that of LipenV two anions, two cations, and two water molecules per asymmetric unit, and those of KpenV and RbpenV four anions and four cations. All five structures are similar in the molecular packing motif within the crystals, but the only isomorphism is

(16) Pines, A.; Gibby, M. G.; Waugh, J. S. *J. Chem. Phys.* **1973**, *59*, 569−590. Yannoni, C. S. *Acc. Chem. Res.* **1982**, *15*, 201−208.
(17) Stejskal, E. O.; Schaefer, J. *J. Magn. Res.* **1975**, *18*, 560−563.
(18) Tegenfeldt, J.; Haeberlen, U. *J. Magn. Res.* **1979**, *36*, 453−457.
(19) Earl, W. L.; VanderHart, D. L. *J. Magn. Reson.* **1982**, *48*, 35−54.
(20) Opella, S. J.; Frey, M. H. *J. Am. Chem. Soc.* **1979**, *101*, 5854−5856.
(21) Harbison, G. S.; Smith, S. O.; Pardoen, J. A.; Courtin, J. M. L.; Lugtenburg, J.; Herzfield, J.; Mathies, R. A.; Griffin, R. G. *Biochemistry* **1985**, *24*, 6955−6962.
(22) Torchia, D. *J. Magn. Reson.* **1978**, *30*, 613−616.
(23) Twyman, J. M.; Dobson, C. M. *Magn. Reson. Chem.* **1990**, *28*, 163−170.
(24) Conner, C.; Naito, A.; Takegashi, K.; McDowell, C. A. *Chem. Phys. Lett.*, **1985**, *113*, 163−170. Takegashi, K.; McDowell, C. A. *J. Am. Chem. Soc.* **1986**, *108*, 6852−6857.
(25) Jeener, J.; Meier, B. H.; Bachmann, P.; Ernst, R. R. *J. Chem. Phys.* **1979**, *71*, 4546−4553.
(26) Bushweiler, C. H.; Letendre, L. J.; Brunelle, J. A.; Bilotsky, H. S.; Whalon, M. R.; Fleischmann, S. H. Quantum Chemistry Program Exchange Program, Program No. 466, DNMR4.
(27) Rothwell, W. P.; Waugh, J. S. *J. Chem. Phys.* **1981**, *74*, 2721−2732.

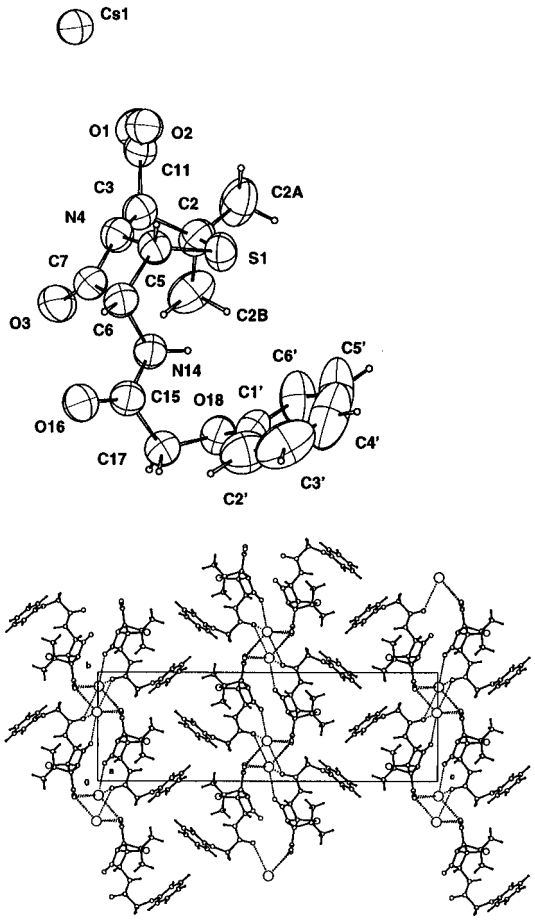

Figure 1. The crystal structure of CspenV shown in projection down *a*, together with a drawing of the molecule in the same orientation, in which the atoms are represented by their 50% atomic displacement ellipsoids.

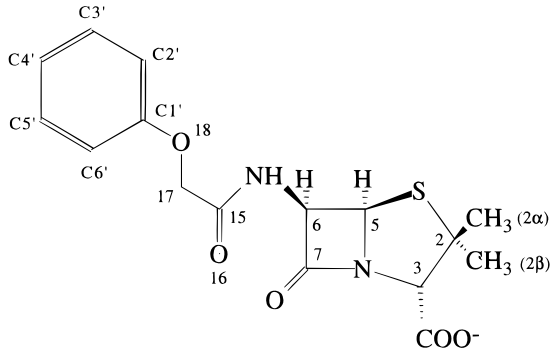

1

that of KpenV and RbpenV. CspenV is in fact isostructural with potassium benzylpenicillin (KpenG)[28,29] and NapenV is isostructural with sodium benzylpenicillin (NapenG).[28]

i. The Molecular Structure of the PenV Anion. The bonded distances and interbond angles in the penV anions in the Li, Na, and Cs salts are presented in the Supporting Information and in most respects show no significant differences from those reported for KpenV[1a] and HpenV.[7] In all nine independent molecules of the five MpenV crystal structures the thiazolidine ring has a C-3 conformation;[4] that is with the

(28) Crowfoot, D.; Bunn, C. W.; Rogers-Low, B. W.; Turner-Jones, A. In *The Chemistry of Penicillin*; Clarke, H. T., Johnson, J. R., Robinson, R., Eds.; Princetown University Press, New Jersey, 1949; pp 310−366.

(29) Prout, K.; Baird, P.; Crook, S. M.; Watkin, D. J.; Twyman, J. M.; Heyes, S. J.; Dobson, C. M. Unpublished results.

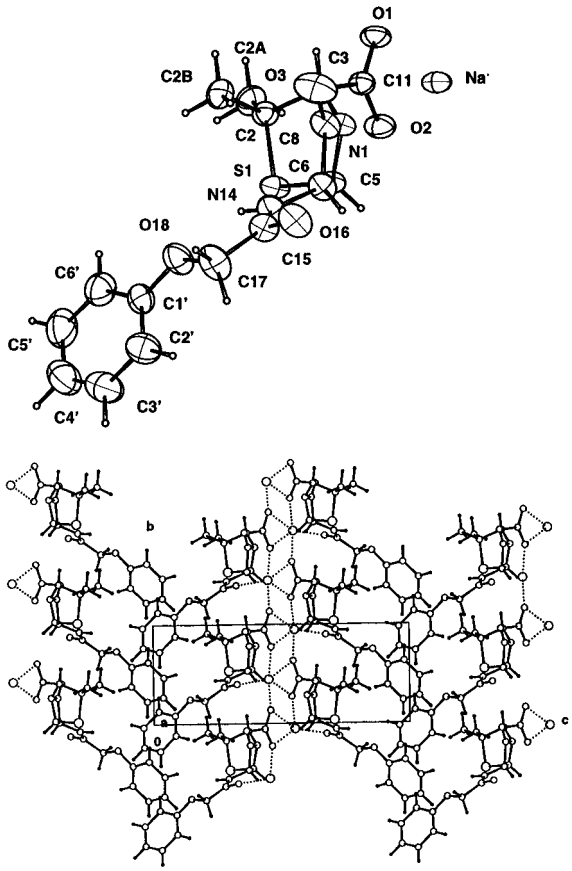

Figure 2. The crystal structure of NapenV shown in projection down *a*, together with a drawing of the molecule in the same orientation, in which the atoms are represented by their 50% atomic displacement ellipsoids.

α-CO_2H group axial. The fused-ring *β*-lactam/thiazolidine system appears very rigid so that the only significant differences between the nine molecules lie in the orientation of the phenoxy side chain with respect to the bicyclic ring system. These differences are emphasized in Figure 5 and Table 2, which lists for each molecule the five torsion angles which describe the side chain conformations. Three of these torsion angles, C5−C6−N14−C15, C6−N14−C15−C17, and N14−C15−C17−O18, are very similar at 180 ± 15° for all nine conformers. Thus the amide bond is *trans*, and the N−H proton must form an intramolecular hydrogen bond with the ether oxygen atom. Ignoring the H atoms, the chain of atoms from C5 to O18 is coplanar with two *trans* linkages and a final *cis* linkage. Relative to this planar extended chain of atoms the phenyl group occupies a wide variety of positions, indicating that there is no single conformation with a significantly lower intramolecular energy than the rest. In the structure of LipenV the two independent molecules in the asymmetric unit have very similar side chain conformations, but in KpenV (RbpenV) there are four very different orientations of the phenyl group.

ii. Molecular Packing within the Crystal Structures. The crystals have layer structures composed of stacks of molecular sandwiches. Each sandwich has a hydrophilic interior with a layer of cations (and, in the case of LipenV, water molecules) at the center coordinated by the penV oxygen atoms. The hydrophobic phenyl groups of the side chains constitute the surfaces of these sandwiches. In each crystal these sandwiches are parallel to the *ab* plane. The *c* axis repeat is either one sandwich (HpenV, NapenV, KpenV, and RbpenV) or two sandwiches (LipenV and CspenV) related by a 2-fold screw axis. The interlayer separations fall into two groups, depending

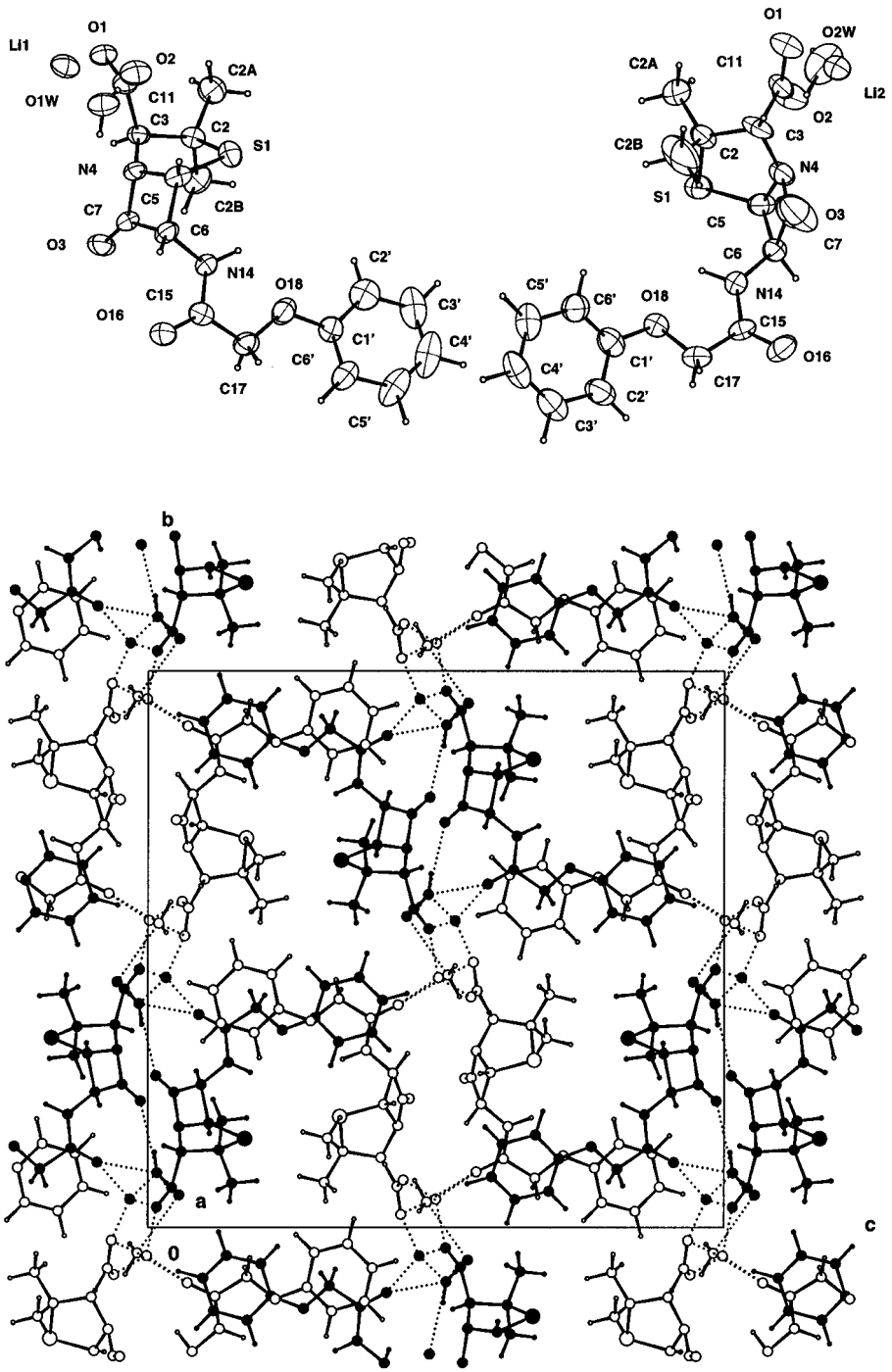

Figure 3. The crystal structure of LipenV shown in projection down *a*, together with a drawing of the two molecules in the same orientation, in which the atoms are represented by their 50% atomic displacement ellipsoids. Molecule 1, the molecule associated with Li1, is drawn in black in the structure diagram, and molecule 2, associated with Li2, is drawn with open circles.

on whether the phenyl groups of adjacent sandwiches just touch (CspenV, $d_{002} = 15.005$ Å; RbpenV, $d_{001} = 15.145$ Å; KpenV, $d_{001} = 15.150$ Å and NapenV, $d_{001} = 15.795$ Å) or interleave (LipenV, $d_{002} = 11.338$ Å; HpenV, $d_{001} = 12.06$ Å) (Figures 1−4).

The orientation of the fused-ring β-lactam/thiazolidine system is determined by the number of oxygen atoms required to satisfy the cation coordination. In the structure of CspenV the Cs^+ ion is coordinated by seven oxygen atoms, one β-lactam, two amide, and four carboxylate oxygens from six neighboring penV anions, Figure 1, and is very similar to but not the same as the coordination of K^+ in KpenV.[1a] In NapenV the Na^+ ion is coordinated by five oxygen atoms (Figure 2). In LipenV the penV anions interact with a mixed layer of Li^+ ions and water molecules (Figure 3). Each Li^+ ion is coordinated by four oxygen atoms, one amide oxygen, two carboxylate oxygens from three penV anions, and an oxygen atom of a water molecule, and each water molecule coordinates one Li^+ ion. The water molecule oxygen atom O(1) H-bonds to the carboxylate O(102) and the β-lactam oxygen O(103), O(2) H-bonds only to carboxylate oxygen atom O(201). The HpenV structure follows the same general principles of a molecular sandwich with a hydrophobic exterior and a hydrophilic middle. The basic unit is, however, a chain with the carboxylate hydroxyl of one molecule H-bonded to the side chain amide oxygen of the molecule translated one unit cell along *b*. C-centering extends the chains into sheets and the 2-fold axes the sheets into sandwiches.

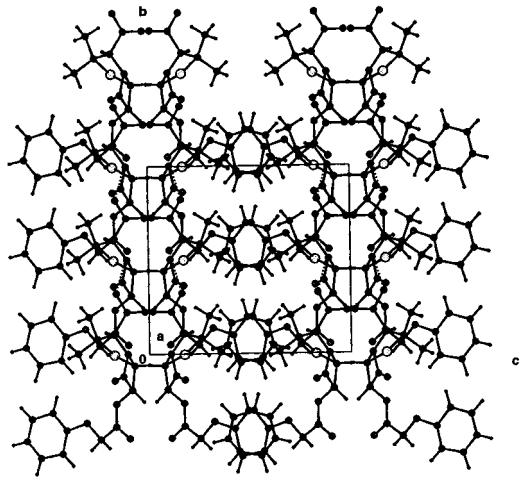

Figure 4. The crystal structure of HpenV shown in projection down *a*. The coordinates used are those of Abrahamsson *et al.*,[7] inverted to give the correct enantiomer. The molecular packing arrangement leads to hydrogen-bonded molecular chains parallel to *b*.

iii. Anisotropic Displacement Parameters. The atomic displacement ellipsoids (Figures 1−3 for the Cs, Na, and Li salts) of the atoms of the phenoxy groups show no evidence for any disorder. The ellipsoids may be viewed both in projection on to and perpendicular to the plane of the phenoxy group, Figure S2. In two structures (KpenV and CspenV) larger amplitude in-plane librational motion is suggested, but there is little significant difference (except perhaps for molecule 3 of the KpenV structure) in the out-of-plane motion. For LipenV the ring of anion 1 has larger in-plane components to its thermal motion than that of anion 2.

b. ^{13}C CP/MAS NMR Spectroscopy. ^{13}C CP/MAS NMR spectra of HpenV, LipenV, NapenV, RbpenV, and CspenV at ambient temperature are shown in Figure 6. The spectra show well-resolved, widely dispersed resonances of good signal-to-noise ratio; bands of resonances from carbon atoms of distinct functional groups can be identified immediately. Detailed assignments were made as discussed previously for KpenV,[1a] by identifying ^{13}C resonances of quaternary and mobile carbon atoms from NQS experiments,[20] and carbon atoms bonded directly to nitrogen by their characteristic asymmetric doublets,[30] and by comparison with spectra of structurally related compounds,[4,31] particularly KpenV.[1a]

i. CspenV. In the ambient temperature spectrum of CspenV (Figure 6f) the very sharp well-resolved lines in the upfield region, notably those of the 2α- and 2*β*-methyl groups,[4] are clearly evident. Only a single resonance is apparent for each resolved carbon site, indicating that the crystals contain one molecule in the asymmetric unit. The aromatic region shows only two sharp resonances, which are assigned to the *ipso* C1′ and *para* C4′ carbons, and two very broad resonances which are assigned to the remaining four aromatic carbon sites. Similar spectra have been observed before for penicillins, specifically KpenV,[1a] sodium carfecillin,[32] and KpenG.[29] This pattern is interpreted as indicative of a 180° flip motion of the phenyl rings about their local 2-fold axes and has been discussed in detail in respect of KpenV.[33]

The variation with temperature of the aromatic region of the ^{13}C CP/MAS NMR spectrum in the temperature range 210−345 K is given in Figures 7a and S3; other regions of the spectrum are essentially temperature independent.[34] In the spectrum at 213 K separate C2′ and C6′ aromatic carbon resonances are clearly resolved, but the C3′,C5′ resonances are degenerate. As the temperature is increased above 213 K the resonances of the inequivalent *ortho* carbons C2′,C6′ of the phenyl ring display classic two-site exchange broadening, with coalescence at 235 K and subsequent resharpening to give a single well-defined resonance. For the resonances of the C3′,C5′ sites, whose frequency separation is too small to be observed, only slight line-broadening can be seen to occur over this temperature range. Despite initial sharpening of the averaged C2′,C6′ resonance above 237 K, it and the C3′,C5′ resonance both broaden dramatically above ∼244 K, reaching maximum line width at 282 K before resharpening to their limiting high-temperature line width by 340 K. This behavior is interpreted as the motional rate of the ring flip process moving initially into the MAS broadening regime[35] and then subsequently at higher temperatures into the dipolar broadening regime.[27]

The observation of the temperature-dependent behavior of the aromatic resonances in the ^{13}C CP/MAS NMR spectrum arising as a consequence of the phenoxy ring reorientation provides an opportunity to extract quantitative kinetic information and activation parameters. The results of three independent and complementary techniques, chemical exchange lineshape analysis, dipolar broadening analysis and magnetization transfer experiments, were obtained from studies of CspenV. Between 205 and 225 K exchange is too slow to result in significant lineshape changes, but the kinetic behavior was studied by ^{13}C CP/MAS magnetization transfer experiments[24] between the C2′ and C6′ resonances.

Between 213 and 244 K chemical exchange broadening of the C2′,C6′ resonances is evident, and rate constants were determined by comparison of the experimental spectra with calculated lineshapes (DNMR4, QCPE 466[26]) (Figure S4). The rate data fit an Arrhenius rate law with an activation energy of 84.7 kJ mol^{-1} and a frequency factor of 7.5×10^{21} s^{-1}. The rates at 241 and 244 K deviate from linearity, as the contributions to the line widths from MAS broadening become significant.

Above 282 K in the short correlation time regime of the the dipolar broadening interaction, where the effects of exchange broadening are negligible, the line broadening was analyzed to provide additional rate data. The deconvoluted line widths, $\Delta\nu_{1/2}' = \Delta\nu_{1/2} - (\Delta\nu_{1/2})_o$, of both exchange-averaged isotropic resonances, (C2′,C6′) and (C3′,C5′), were measured, and $\ln(\Delta\nu_{1/2}')$ for each was plotted against the inverse temperature. Fits to the theory of Rothwell and Waugh[27] yield activation barriers of 68.8 and 65.5 kJ mol^{-1} for C2′,C6′ and C3′,C5′ respectively, (Figure 8). These values are consistent and indicate well-defined Arrhenius behavior.

The rate constants determined from the three independent analyses are plotted together in Figure 9 and combined analysis yields activation parameters of $E_a = 72 \pm 10$ kJ mol^{-1} and $A_o = (1.3 \pm 1) \times 10^{19}$ s^{-1}.

(30) Hexem, J. G.; Frey, M. H. Opella, S. J. *J. Am. Chem. Soc.* **1981**, *103*, 224−226. Hexem, J. G.; Frey, M. H. Opella, S. J. *J. Chem. Phys.* **1982**, *77*, 3847−3856.

(31) Twyman, J. M.; Dobson, C. M. *J. Chem. Soc., Chem. Commun.* **1988**, 786−788. Twyman, J. M. D. Phil Thesis, University of Oxford, 1989.

(32) Twyman, J. M. D. Phil Thesis, University of Oxford, 1989. Wendeler, M.; Heyes, S. J. Unpublished results.

(33) The pattern of nuclear exchange indicated by magnetization transfer experiments; the observation of pairwise exchange broadening and coalescence of certain phenyl resonances; the extent of the averaging of chemical shift anisotropy (CSA) indicated with rise in temperature; the observation of an extensive ^{13}C−^{1}H dipolar broadening regime; the absence of any positional disorder in the X-ray crystal structures−all these observations are consistent with 180° ring flip motions as the single most significant dynamic process in these crystals.

(34) On lowering the temperature below 220 K the methyl resonances broaden progressively. This is interpreted as the methyl group C_3-reorientation slowing into the dipolar broadening regime.[27]

(35) Suwelack, D.; Rothwell, W. P.; Waugh, J. S. *J. Chem. Phys.* **1980**, *73*, 2559−2569.

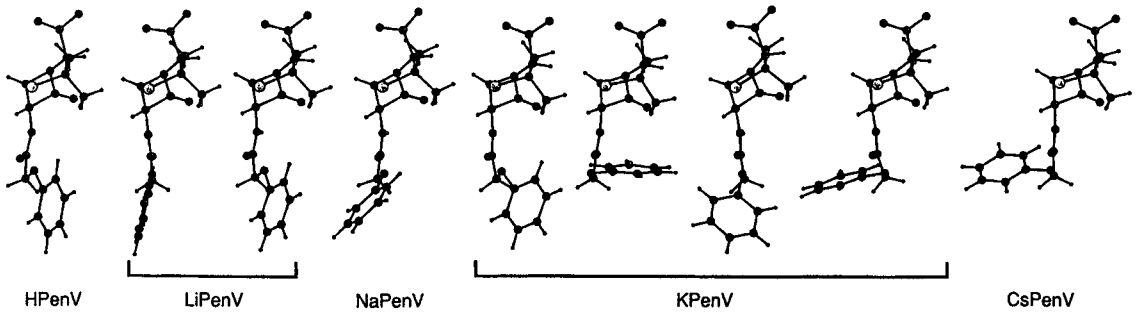

Figure 5. The nine penV anion conformations observed in the crystal structures of (from left to right) HpenV, LipenV (two molecules), NapenV, KpenV (four molecules), and CspenV, illustrating the observed conformational variability of the phenoxy portion of the side chain and the similarity and apparent conformational rigidity of the penam nucleus. The relevant torsion angles are listed in Table 2.

Table 2. Selected Torsion Angles Referred to Atom Numbering on the NMR Convention Presented in **1**

	atoms			
angles	1	2	3	4
A	C5	C6	N14	C15
B	C6	N14	C15	C17
C	N14	C15	C17	O18
D	C15	C17	O18	C1′
E	C17	O18	C1′	C6′

molecule		A, deg	B, deg	C, deg	D, deg	E, deg
HpenV		−155.6	170.5	5.1	160.8	15.3
LipenV	1	−178.6	176.5	5.1	174.4	16.7
	2	−161.2	179.5	6.5	−168.0	2.3
NapenV		162.4	−165.2	−14.3	161.2	−14.7
KpenV (293 K)	1	173.6	172.3	−1.2	−160.0	−51.5
	2	168.7	−176.2	8.4	−86.7	0.4
	3	165.5	−178.0	11.0	161.0	77.3
	4	178.5	171.6	12.8	87.0	3.2
CspenV		172.3	−179.7	13.3	89.1	25.0

ii. RbpenV. The ambient temperature ^{13}C CP/MAS NMR spectrum of RbpenV (Figure 6e) is very well-resolved, but is considerably more complex that that of CspenV, resembling closely the spectrum of KpenV.[1a] The changes in the spectrum with temperature (Figure S6) also parallel those observed and analyzed in detail previously for KpenV.[1a] They indicate that RbpenV, like KpenV, has a low temperature phase with a complex crystal structure having four molecules in the asymmetric unit. At ∼355 K a phase change occurs to a structure with two molecules in the asymmetric unit.

The aromatic region of the spectrum at 202 K (Figures 7b and S7) shows C2′,C6′ and C3′,C5′ aromatic carbons of all four molecules in the asymmetric unit to be averaged into the fast limit of the exchange-broadening time scale by ring flip processes. As the temperature is raised above 202 K, these resonances broaden gradually to the limits of observability at ∼240 K and then begin to narrow, becoming fully resharpened by 296 K. In contrast to CspenV, therefore, the aromatic ring motions of RbpenV could not be frozen out into the slow exchange limit at the lowest temperature accessible to us. This fact, and the observation that maximum dipolar broadening occurs at ∼240 K in comparison with 282 K for CspenV, is indicative of a faster rate of ring flip at a given temperature for RbpenV than CspenV. RbpenV shows similar rates of ring flip to KpenV,[1a] but in contrast to KpenV the identical broadening behavior of the different resolved C2′,C6′ resonances indicates the phenoxy rings of the four crystallographically inequivalent molecules to have essentially identical dynamic behavior. Analysis of the dipolar line broadening in the short correlation time regime above 278 K indicates an Arrhenius activation barrier of $E_a = 51 \pm 4$ kJ mol^{-1}. Substitution of the known rate of exchange ($k = 9.4 \times 10^5$ s^{-1}) at the temperature of maximum broadening (240 K) yields a preexponential factor of $A_o = 9.1 \pm 3 \times 10^{16}$ s^{-1}.

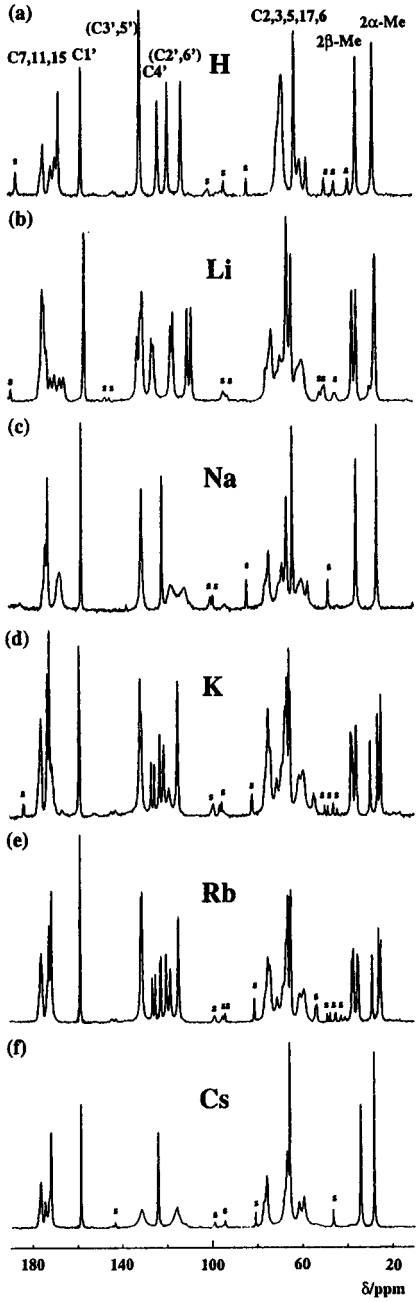

Figure 6. Ambient temperature (296 K) ^{13}C CP/MAS NMR spectra, with annotated assignment, for crystalline samples of (a) HpenV, (b) LipenV, (c) NapenV, (d) KpenV, (e) RbpenV, and (f) CspenV (s denotes spinning sidebands).

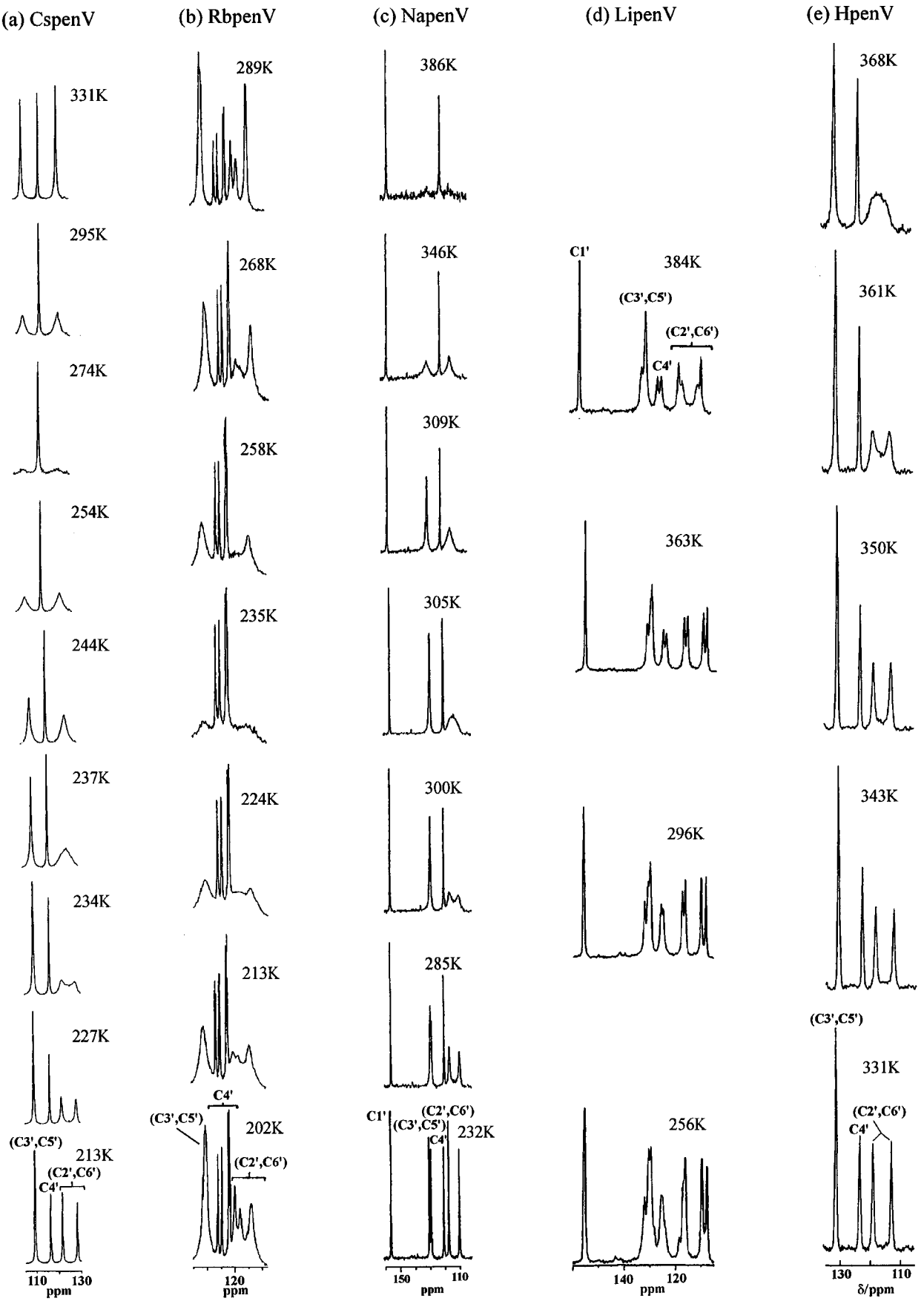

Figure 7. Parts of the aromatic regions of the ^{13}C CP/MAS NMR spectra of (a) CspenV, (b) RbpenV, (c) NapenV, (d) LipenV, and (e) HpenV at selected temperatures. For LiPenV care was taken to ensure that the salt was in the fully hydrated form.

iii. NapenV. The ambient temperature spectrum of NapenV (Figure 6c) like that of CspenV shows broadening effects due to aromatic ring dynamics and also indicates the presence of only one molecule in the asymmetric unit. The ^{13}C CP/MAS spectrum for the aromatic region in the temperature range 232−386 K (Figures 7c and S5) shows discrete resonances at ≤268

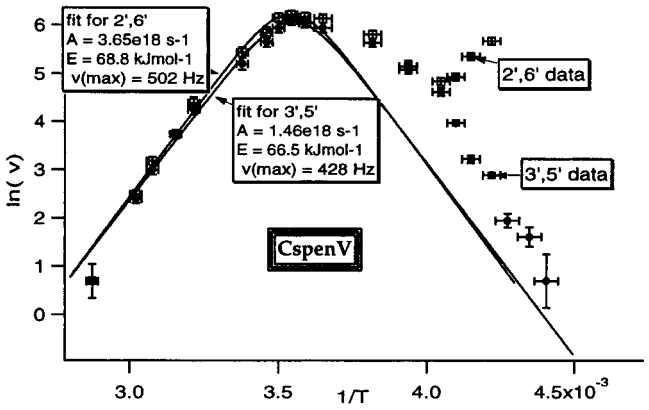

Figure 8. Plots of $\ln(\Delta\nu_{1/2}')$ vs $(1/T)$, where $\Delta\nu_{1/2}'$ is the difference between the measured and limiting (200 K) line widths, for C2′,C6′ and C3′,C5′ resonances of the ^{13}C CP/MAS NMR spectra of CspenV. Both resonances show behavior typical of a reintroduction of dipolar broadening, and at lower temperatures (longer correlation times) both sets of line width data show the affects of MAS broadening, and the C2′,C6′ additionally, and more dramatically, exchange-broadening phenomena. Solid lines represent for each data set a fit, by a least-squares, error-weighted procedure, to the theory of Rothwell and Waugh,[27] restricted to data in the region of maximum broadening and at higher temperatures into the short correlation time regime. In principle the entire C3′,C5′ data set could be fit to a combination of dipolar and MAS broadening expressions, but in practice there is little to gain from this approach. The dipolar broadening data are incorporated into the Arrhenius fit to the composite rate data from the various experiments responding to the different timescales (Figure 9) by conversion of the line widths to rate constants, with an accuracy influenced primarily by the accuracy of the estimation of the temperature of maximum dipolar broadening achieved through the above fit.

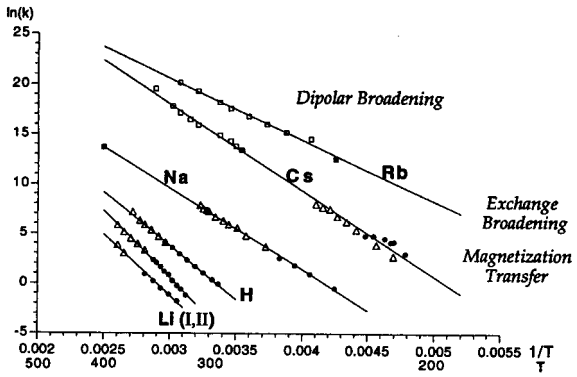

Figure 9. Combined Arrhenius plots for HpenV, LipenV, NapenV, RbpenV, and CspenV, with rate constant data derived from magnetization transfer experiments (●), chemical exchange line shape simulations (△) and dipolar broadening analysis (□). The filled boxes (■) correspond to the points of maximum broadening. The solid lines indicate Arrhenius relationships derived from fits, weighted according to the estimated experimental errors (not indicated on this plot). Li(I,II) indicates the two independent molecules in LipenV. There was no differentiation in the dipolar broadening of the various C2′,C6′ resonances of the four independent molecules of RbpenV, so a single set of rate data is shown—that from the most upfield of the resonances, at ca. 114 ppm.

K for each of the six inequivalent aromatic carbon atoms. As the temperature is increased above 268 K, both the C2′,C6′ and C3′,C5′ carbon resonances of the phenyl ring display classical two-site exchange lineshape changes with coalescence at 285 K for C2′,C6′ and at 305 K for C3′,C5′. Above these temperatures the averaged resonances initially sharpen, but beyond 324 K they broaden again progressively with increase in temperature until at 386 K they are barely resolved from the baseline. Rates of the ring flip exchange process (Figure 9)

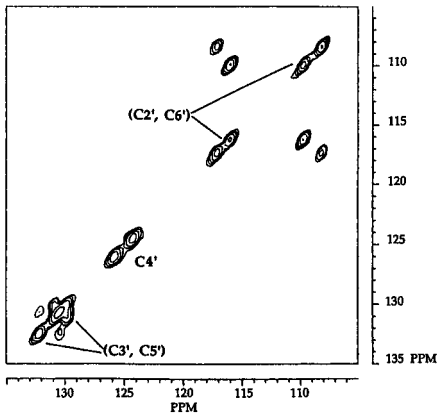

Figure 10. Principal aromatic region of a rotationally asynchronous phase-sensitive ^{13}C CP/MAS 2-D exchange experiment (MAS rate ν_r of 3.95 kHz, ^{1}H rf decoupling field $\nu_{1H} = 55$ kHz, 512 t_1 increments of 108 μs, and a mixing time of 1.0 s) on LipenV, performed at 343 K, and showing strong magnetization transfer between the inner pair of C2′, C6′ resonances and less intense cross peaks between the outer pair of C2′,C6′ resonances. This suggests that the rate of ring flips is different for the two inequivalent molecules in the structural asymmetric unit. The C3′,C5′ region also shows cross peak structure, but the smaller spread in chemical shift leads to poorer resolution of the individual cross peaks.

were determined from exchange-broadened lineshape simulations in the temperature range 268−309 K (Figure S4) and magnetization transfer data measurements in the range 232−261 K for the C2′,C6′ resonances. Arrhenius behavior is found over the entire temperature range with an activation energy for the phenoxy ring flips of 68 ± 3 kJmol^{-1} and a frequency factor A_o of $(7.1 \pm 5) \times 10^{14}$ Hz.

iv. LipenV. In the ambient temperature spectrum of LipenV·H_2O (Figure 6b), the methyl carbon resonances in the upfield region of the spectrum show particularly clearly two peaks for each of the 2α- and 2β-methyl carbon atoms. This indicates that the crystals contain two molecules in the crystallographic asymmetric unit. Similar splittings are evident in the aromatic region; two pairs of C2′,C6′ aromatic resonances arising from the two molecules are clearly resolved at 296 K. At ≥377 K[36] the inner pair of the C2′,C6′ lines broadens and loses intensity (Figures 7d and S8) while the outer two peaks remain sharp; the C3′,C5′ resonance region also shows some broadening. Even at the maximum temperature studied, 384 K, the rate of aromatic ring motion is evidently too slow to result in coalescence and eventual resharpening of exchange-averaged resonances, as seen in the spectra of the other salts discussed above.

A ^{13}C CP/MAS 2D exchange experiment[23] with a mixing time of 1 s performed at 343 K (Figure 10) reveals strong magnetization transfer between the inner pair of C2′,C6′ resonances and less intense cross peaks between the outer pair of C2′,C6′ resonances. These observations are consistent with slow ring flip motions, occurring at different rates for the two molecules in the asymmetric unit. The dynamic behavior was probed by variable mixing time 1D magnetization transfer experiments over the temperature range 325−365 K and by lineshape analysis from 365−384 K. The derived rate data

(36) On heating LipenV·H_2O much above 340 K for significant periods of time an additional set of peaks became evident in the ^{13}C CP/MAS NMR spectra (Figure S1) at increasing intensity with time. Thermogravimetric analysis (TGA) under a flowing argon atmosphere indicated loss of crystal water above the same temperature, to an extent dependent on the duration of the heating and the sample temperature. Placing material that had been heated in this manner in air at ambient temperature overnight resulted in full recovery of crystal water molecules, as shown by the ^{13}C CP/MAS NMR spectrum, which is identical to that of the sample prior to heating.

Table 3. Arrhenius Parameters and Structural Data for Phenyl Ring Flips in PenV Salts

PenV Salt	E_a, kJ mol^{-1}	A_o, s^{-1}	C−C short, Å	(C−C short)$_{av}$, Å	phenyl layer width/phenyl units
H	89 ± 3	$(4.4 \pm 5) \times 10^{15}$	3.544	3.636	0.75
Li(1)	111 ± 8	$(4.6 \pm 5) \times 10^{17}$	3.387	3.567	0.0
Li(2)	102 ± 15	$(2.7 \pm 5) \times 10^{15}$	3.465	3.728	0.0
Na	68 ± 3	$(7.1 \pm 5) \times 10^{14}$	3.672	3.748[5]	1.25
Rb	51 ± 4	$(9.1 \pm 3) \times 10^{16}$			1.75
Cs	72 ± 10	$(1.3 \pm 1) \times 10^{19}$	3.720	3.766[5]	1.5

(Figure 9) fit simple Arrhenius models; activation parameters of E_a 102 ± 15 kJ mol^{-1} with $A_o = (2.7 \pm 5) \times 10^{15}$ s^{-1}, and $E_a = 111 \pm 8$ kJ mol^{-1} with $A_o = 4.6 \pm 5 \times 10^{17}$ s^{-1} for the two distinct molecules.

v. HpenV. The ambient temperature spectrum of the free acid HpenV (Figure 6a) indicates a single molecule in the asymmetric unit. Two narrow, well-resolved resonances are observed from the C2′,C6′ phenoxy sites, between which strong magnetization transfer is observed in a ^{13}C CP/MAS 2D exchange experiment[23] with a mixing time of 2 s performed at 297 K (Figure S10). This indicates phenoxy ring flips in HpenV at a rate in the slow limit of the exchange broadening regime at this temperature. At ≥ 340 K (Figures 7e and S9), the (C2′, C6′) phenoxy line widths increase, in the manner of a classical exchange broadening, with coalescence at 365 K, initial sharpening of the averaged resonance before broadening again at the highest temperature measured, 380 K. Simulation of the exchange-broadened line shapes between 329 and 365 K (Figure S9), and variable-temperature 1D-magnetization-transfer experiments in the temperature range 307−335 K yield ring flip rates which follow Arrhenius behavior with an activation barrier of $E_a = 89 \pm 3$ kJ mol^{-1} and a frequency factor of $A_o = (4.4 \pm 5) \times 10^{15}$ s^{-1}.

Discussion and Conclusions

One hundred eighty degree flip motions of the aromatic rings have been detected by ^{13}C CP/MAS NMR in the temperature range 200−380 K for *all* the penV salts studied here. In each case the rate data can be fitted successfully to Arrhenius relationships (Figure 9 and summarized in Table 3). At any given temperature the flips occur at very different rates in the different salts. For example, at 340 K the same fundamental motion, 180° ring flips, is measured in CspenV with $k = 3.6 \times 10^8$ s^{-1} through dipolar broadening effects and in LipenV with $k = 0.5$ s^{-1} through magnetization-transfer experiments. At ambient temperature measured and predicted (from Arrhenius behavior) rates cover 11 orders of magnitude. Only for CspenV are full data in three motional regimes (magnetization transfer, exchange broadening and dipolar broadening) available. Linearity is, however, observed for the NapenV data over a similarly wide temperature range, and the fits over more restricted temperature regimes for HpenV, LipenV, and RbpenV are no less convincing.

The observation of Arrhenius behaviour at all temperatures and timescales is very striking. Given the changes that occur in a typical molecular crystal through this temperature range, including overall expansion of the crystal (estimated, from typical organic molecular crystal data as indicated by Dunitz[37] and from our own variable-temperature single-crystal X-ray study of KpenG,[29] to be of the order of a 2% change in volume) it is remarkable that simple Arrhenius behavior is observed. Expansion of the unit cell with increase in temperature would be imagined to lead to a decrease in the energy barrier to a spatially demanding motion such as a phenyl ring flip, and the activation barrier should be temperature dependent.

X-ray structure analysis shows that the Li^+, Na^+, K^+, Rb^+, and Cs^+ salts of penV and the free acid exhibit a wide variety of crystal structures (only KpenV and RbpenV are isomorphous). The penam unit is structurally rigid and adopts an almost identical C-3 conformation consistently throughout the penV structures. The phenoxymethyl side chain shows an extremely wide range of conformations with respect to the penam unit. Although by this measure the side chain seems to be remarkably flexible, only in the high temperature forms of K and RbpenV is there significant motion of the side chain between alternative conformations. The adoption of a specific side-chain conformation appears to be driven by the need, in a given structure, for the packing arrangements to satisfy other structural criteria, such as a preferred coordination environment of the cation (see below). The activation barrier to ring flips is not expected to have a significant intramolecular contribution, and indeed there is no obvious direct relationship between the side chain conformation (any or all of the torsional angles listed in Table 2) and flip rates or Arrhenius activation energy to ring flip. However, the molecules with the most compact conformations, CspenV and two of the K(Rb)penV conformers, are those that show the most rapid ring flips at typical temperatures, and the most elongated conformations (e.g., molecule 1 of LipenV) tend to show the highest activation barriers to ring flips. It should be noted that the four different molecules of the RbpenV structure show widely differing torsion angles, but NMR indicates very similar ring flip dynamics for each.

The crystal structures of all the salts and the free acid have the same basic packing motif, the exact form of which appears to be determined by the coordination requirements of the cation (or, for the free acid and partially for LipenV hydrate, H-bonding). The structural theme is that of a molecular sandwich with a hydrophilic core and a lipophilic surface. All the structures can be considered as comprising of layers that are two molecules in thickness. All structures contain regions in which electrostatic interactions between the cations and oxygen atoms dominate intermolecular interactions and other regions with primarily van der Waals interactions. It is within the layers that strong Coulombic forces dominate the structural arrangement, but adjacent layers interact only through much weaker dispersion forces. The principal change in the series of crystals is a systematic variation in the radius of the atomic countercation to the penV anion from H^+, through Li^+, Na^+, K^+, and Rb^+ to Cs^+. With the increase in size of the cation the number of ligator atoms at the cation increases from 2 to 7, thus increasing the number of penV oxygen atoms that engage the cation and so changing the orientation of the anion with respect to the plane of the sandwich structure. In one respect these structures are alike: they all have a rigid ionic core with increasing molecular motion toward the lipophilic surface. The increased motion is indicated by increasing XRD adps toward the lipophilic surface and the consistent observation of 180° flips of the phenyl rings

(37) Dunitz, J. D. *X-Ray Analysis and the Structure of Organic Molecules*, 2nd ed., 2nd repr.; VCH: Weinheim, 1995.

from the ^{13}C CP/MAS NMR, albeit at flip rates that span orders of magnitude at a given temperature.

The ring flip event does not lead to positional disorder and so is essentially diffraction invisible. The adps of the phenyl ring atoms in the crystal structures relate to the extent of the faster ($t \approx 10^{-15}$ s) vibration of the atoms and librational motions of the phenyl groups. Previous studies have shown that the phenoxy and benzyl rings of penicillin V benzyl ester or of its β-sulfoxide have very different ring flip rates and Arrhenius activation parameters.[31] Yet, single-crystal X-ray studies at ambient temperature and also at 143 K for the β-sulfoxide[38] show very similar adps for phenoxy and benzyl rings at a given temperature, thus suggesting that there is no specific correlation between librational amplitudes and the rates of the slower, activated ring flip process. TLS analyses[39] of the adps of the phenoxy groups of NapenV, and CspenV and molecule 2 of LipenV are consistent with rigid body motion, but that of molecule 1 of LipenV is not. On the grounds of the nature of its closest contacts the phenyl ring of molecule 1 may be judged the ring most "entrapped" in any of these structures, and is thus the least likely to undergo ring flip motion. The maximum librational amplitude is greatest for CspenV and is approximately equal for LipenV (molecule 2) and NapenV. The libration analysis for CspenV is consistent with that for the isostructural KpenG (benzyl penicillin) for which variable-temperature single-crystal XRD data are available and have been analyzed in detail.[29]

Looking in detail at the local environment of the structures, in LipenV, which has the lowest flip rates and the highest activation barriers, the phenyl groups lie between pairs of amide groups of penV anions from the other molecule type in the asymmetric unit, in the neighboring layer. Deformation of the surroundings is likely to be difficult, explaining the relatively slow rates of ring flips. HpenV also has a low rate of and a high activation barrier to ring flips, and in this structure it is the C2-methyl groups of molecules from a neighbouring layer that provide the most rigid obstacle to flips. In the NapenV structure, the extended conformation of the side chains leads to the closest contacts to a phenyl ring being to atoms of the phenyl rings of molecules in the adjacent layer. In addition, the C_2 axes of adjacent rings are oriented at ~90° to each other in a plane orthogonal to the layers. This offers adjacent rings a better opportunity to be displaced to enable a neighboring ring flip event to occur. In the K(Rb)penV and CspenV structures the compact conformation of the penicillin V sidechain leads to closest contacts with methyl groups of the penam unit, either intramolecularly or with those of a molecule in the adjacent layer but the increased size of the cation opens up the contact distances between adjacent phenyl groups within a layer, giving a generally more open structure. There is, therefore a qualitative correlation between the rates of aromatic ring flips and the structure of the crystals in which they are located.

A variety of structural parameters from each penV crystal were examined for possible correlation with the observed ring flip parameters. Some of these parameters do correlate surprisingly well with the propensity for ring flips in the different salts (Figure S11). However, ring flip events clearly occur when the structure has temporarily "opened up" around the ring. It is not surprising then that a single parameter from the equilibrium structure determinations is inadequate to summarize the quality of the local environment of a ring in regard of its encouragement to the nonequilibrium ring flip events. We sought nevertheless to assess the qualities of the molecular packing arrangements that might indicate the relative ease of ring flips in the closely structurally similar set of penicillin crystals. We note that when the phenyl groups of adjacent sandwiches interleave (LipenV and HpenV) the flip rates are low but when the phenyl groups of adjacent sandwiches just touch (CspenV, RbpenV, KpenV, and NapenV) the rate of ring flips is much faster, and of the latter group the ring flips for RbpenV and CspenV, the most open structures, are fastest throughout the temperature range. A similar pattern is found for the activation barriers to ring flip, which are larger for the intercalated than the touching structures. The energy barriers are lower for the more complex, and open, structure of the isomorphous KpenV and RbpenV than for the simpler structures of NapenV and CspenV. Although our conclusion is that these slow, spatially demanding motions are determined by a complex interplay between different structural factors, we find a pleasing correlation of the activation energy to ring flips with the phenyl layer spacings in the structure (Figure 11).

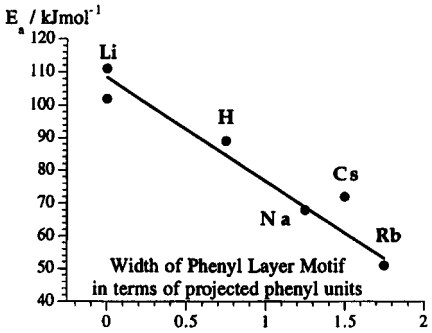

Figure 11. Correlation of the Arrhenius activation barriers, E_a, to phenyl ring flips with a measure of the width of the layer motif of the phenyl groups. The measurement unit is the width of the phenyl ring projected onto the *c* axis and so differs between the various penV salts as a result of different orientations of the plane of the phenyl ring with respect to the lamellar motif. Values are defined only to the nearest 0.25 of a unit. This measurement unit has been adopted with the aim of encapsulating the effects of layer width and relative phenyl ring orientations within a single structural parameter tailored for prediction of ease of ring flip.

We believe that slow motions in molecular crystals of the type discussed in this paper represent a widespread phenomenon and that analysis of the underlying determinants of these motional properties is possible using a combination of NMR and diffraction techniques. The observation of activation parameters for a range of related structures offers an invaluable information source with which to attempt to model the ring flip processes. Such analyses could have substantial implications for our understanding not just of intermolecular interactions within the crystal, but of interactions within and between macromolecular species including synthetic and natural polymers and macromolecules, for which similar motions have been observed.

Acknowledgment. J.M.T. thanks the EPA Cephalosporin and Educational Trusts and Pembroke College for financial assistance. S.J.H. thanks the Glasstone Benefaction for a Fellowship, M.W. thanks the Studienstiftung Deutschlands for a Scholarship, and A.J.E and J.F. thank the SERC for financial support.

Supporting Information Available: Tables of atomic coordinates, atomic displacement parameters, and bond distances and angles and 11 figures referred to in the text as Figures S1−S11 (25 pages). See any current masthead page for ordering and the Internet access instructions.

JA9640657

(38) Baird, P; Twyman, J. M.; Dobson, C. M.; Prout, K. Unpublished results.

(39) Wendeler, M.; Edwards, A. J.; Heyes, S. J.; Prout, K. Unpublished results.